



Effect of Grounded Needles on Electrical Treeing in XLPE Cable Specimens under AC Stress

[Link to publication record in Manchester Research Explorer](#)

Citation for published version (APA):

Hu, F., Rowland, S., Emersic, C., Gardner, R., & Chen, T. (2022). Effect of Grounded Needles on Electrical Treeing in XLPE Cable Specimens under AC Stress. In *International Conference on Dielectrics*

Published in:

International Conference on Dielectrics

Citing this paper

Please note that where the full-text provided on Manchester Research Explorer is the Author Accepted Manuscript or Proof version this may differ from the final Published version. If citing, it is advised that you check and use the publisher's definitive version.

General rights

Copyright and moral rights for the publications made accessible in the Research Explorer are retained by the authors and/or other copyright owners and it is a condition of accessing publications that users recognise and abide by the legal requirements associated with these rights.

Takedown policy

If you believe that this document breaches copyright please refer to the University of Manchester's Takedown Procedures [<http://man.ac.uk/04Y6Bo>] or contact uml.scholarlycommunications@manchester.ac.uk providing relevant details, so we can investigate your claim.



Effect of Grounded Needles on Electrical Treeing in XLPE Cable Specimens under AC Stress

F. Hu, C. Emersic, H. McDonald, L. Chen*, S. Rowland and R. Gardner

Department of Electrical and Electronic Engineering, The University of Manchester, Manchester, M13 9PL, UK

*lujia.chen@manchester.ac.uk

Abstract- Electrical treeing is a pre-breakdown phenomenon which occurs in polymers and can lead to power failure in cables. Common electrode configurations used to initiate tree growth in laboratories use an HV needle and grounded plane, which may be impractical for some experimental situations. This paper investigates the influence of earthing the needle and energizing the planar electrode on electrical treeing characteristics, such as initiation and propagation. Testing was conducted under 50 Hz AC stress, in samples cut from XLPE cables. Experimental parameters such as tree initiation time, growth rate, fractal dimension, and phase-resolved partial discharge (PRPD) patterns were measured. Analysis shows that there is negligible difference in treeing behavior as a result of changing the earthing arrangement, verifying that the experimental arrangements are equivalent.

I. INTRODUCTION

The phenomenon of electrical tree initiation and growth in solid polymer dielectrics can lead to the breakdown of high voltage (HV) insulation equipment. Electrical trees can be described as gas-filled channels, which are thought to initiate from voids and imperfections within the bulk of insulation materials [1]. Phase Resolved Partial Discharge (PRPD) pattern evolution is often used to indicate stages of tree growth [2]. To characterize the density of tree channels, fractal dimension analysis is completed to classify the tree geometry [3].

The majority of previous studies have initiated trees using an HV needle electrode. This produces a highly divergent field, leading to space charge injection and tree initiation. Previous research has shown that tree growth is dependent on factors, such as frequency, magnitude, and voltage waveform [2-3].

In [4-6], authors investigated the influence of different electrode geometries, however, there is little published data investigating the impact of which electrode is earthed in needle-to-plane configurations under AC stress. In DC experiments, the polarity of the needle is critical [9].

While many studies using a needle-to-plane geometry raise the electric potential of the needle, it may be more practical to energize the planar electrode in testing environments with less accessibility for HV needle connections. Under AC, there is no reason to expect a difference in growth behavior when changing the high voltage electrode, apart from the relationship between the electrodes and the surrounding stray capacitance to ground. However, it is not experimentally verified whether this will change tree growth characteristics. Hence, a direct comparison of the two experimental configurations is made in this study.

II. METHODOLOGY

A. Sample Preparation

The metallic sheath and semi-conductive layers were removed from a 66 kV cross-linked polyethylene (XLPE) cable before the insulation was cut into 3 mm thick half-ring samples. To improve the visibility of tree growth, samples were polished using an OmegaPol polishing machine for 5 mins under 250 rpm, with an increasing grit from 600 to 2400. Samples were heated to 140 °C in a vacuum oven for 1 hour before the slow insertion of a 1 mm diameter stainless steel needle with a 3 μm tip radius and 30° tip taper. A 2 ± 0.1 mm spacing was ensured in all tested samples between the needle and plane electrodes. Samples were then left in the heated oven for another hour before 12 hours of passive cooling. Insulating tape was applied around the needle region exposed to open air at the sample-to-needle interface. This was to prevent discharge activity from the interface at a high electric potential.

B. Experimental Setup

Fig. 1 shows the experimental setup. Tree growth was optically imaged every 15 seconds using a Manta G-507B CCD camera and image-capturing software. The voltage source was from a Thurlby Thandar TG215 2 MHz function generator, Europower EP4000 amplifier, and 80 kV_{RMS} transformer.

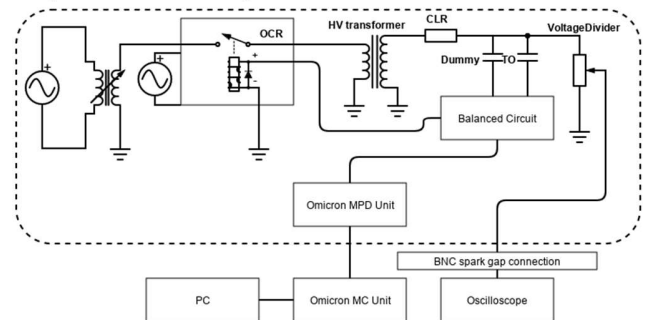


Fig. 1 Experimental test circuit.

A balanced circuit was used for partial discharge (PD) measurements, with an Omicron MPD 800 system in accordance with IEC 60270, to remove the background noise [10]. A PD-free sample was fabricated using a needle with a 500 μm rounded tip, to act as a dummy sample with the test object (TO). The system was calibrated with the Omicron CAL 542 and had a sensitivity of approximately 1 pC.

An overcurrent relay (OCR) and a 500 k Ω rated current-limiting resistor (CLR) were used to protect the test equipment in the event of a breakdown.

A 50 Hz AC power supply was used in all tests. The voltage ramp rate was approximately 500 V_{RMS}/s, where the target voltage was based on an initial peak electric field at the needle tip, calculated using Mason's equation [11]. For a gap distance of 2 mm, the calculated voltage is approximately 7.5 kV_{RMS} and the calculated peak field at the needle tip is 895 kV/mm.

Samples were energized for approximately 2 hours until the tree length had nearly bridged the two electrodes. Breakdown and corresponding material damage were avoided to ensure microscope images of the full tree structure could be analyzed. A Keyence VHX 7100 microscope was used to image tree growth after each test. Detailed analysis was carried out on captured images to calculate bend and bifurcation angles, fractal dimension, and tree growth rate.

III. RESULTS AND DISCUSSION

Two datasets were collected; the first set used an HV needle and a grounded plane configuration, and the second configuration consisted of a grounded needle and an HV plane.

A. Microscope Images

Fig. 2 shows microscope images of trees from both datasets and the total time under the target voltage. Images have been focus-stacked to achieve a deeper depth of field by blending multiple images together.

B. Tree Initiation

Initiation time was measured from the time at which the target voltage was reached, to the time at which the first visible branch was imaged through the CCD camera. Tree initiation time is presented in Table 1 for both cases.

Four of the five samples recorded initiation within 5 mins, with sample 5 taking nearly an hour. Trees grown under a grounded needle had initiation times of at least 14 mins but could also take more than twice as long. The mean initiation time for trees grown using a grounded needle was approximately twice as long for trees grown using a HV needle.

The tree initiation process is inherently stochastic, as reported in [12], and the unpaired t-test gives a p-value of 0.2728. This provides evidence that the longer initiation time is not a direct cause of the needle being grounded. Although, a larger dataset is required for greater statistical confidence.

TABLE I. TABULATED DATA OF INITIATION TIME FOR TESTED SAMPLES

Configuration	Sample	Initiation Time (mins)
HV Needle and Grounded Plane	1	1
	2	2
	3	57
	4	3
	5	5
Grounded Needle and HV Plane	1	18
	2	16
	3	44
	4	14
	5	60

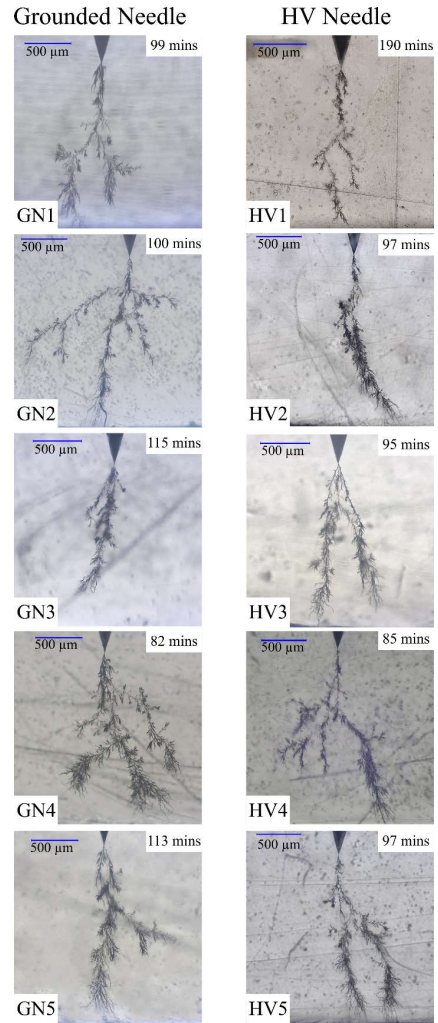


Fig. 2. Focus-stacked microscope images of grounded needle (GN) and high voltage needle (HV) samples labeled with the total tree growth time under the applied field.

C. Tree Growth Rate

The lengths of the electrical trees from the needle tip were measured from the recorded images for every 5 mins of growth. For each image, the length and width of the tree were measured in pixels and then converted into μm . The growth rates of all samples have been plotted in Fig. 3.

All samples with grounded needles reached the stagnant growth period within 15 mins of initiation, with a minimum growth of 400 μm . Samples showed little growth in tree length for at least 20 mins before reaching the second faster growth period. For samples with an HV needle, there was relatively greater variability in the tree length before the growth stagnated. However, this may simply reflect the stochastic nature of tree growth.

Trees from both needle-to-plane configurations show growth rate profiles consistent with those reported in the literature, with fast initial growth, followed by slow or stagnated growth, and eventually leading to runaway [13]. Occasionally, transient rapid growth could occur within the stagnant period of slow growth for samples with an HV needle.

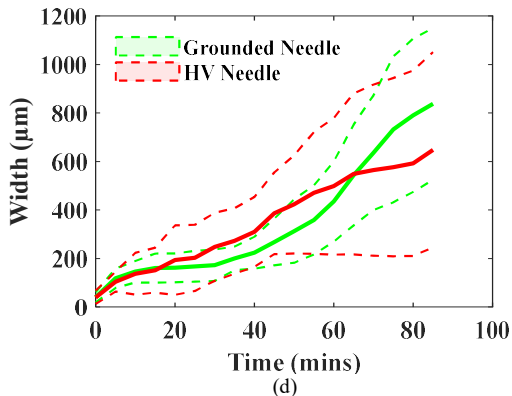
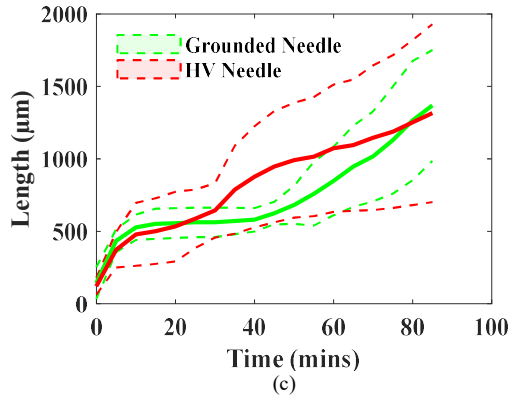
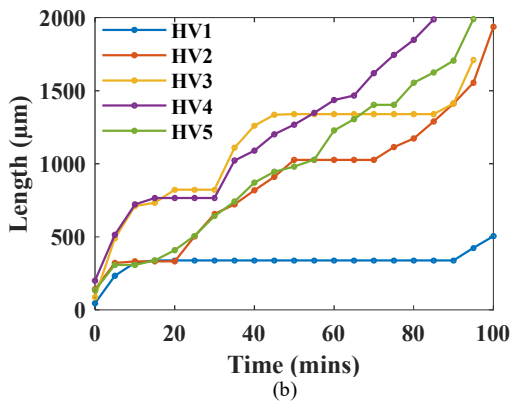
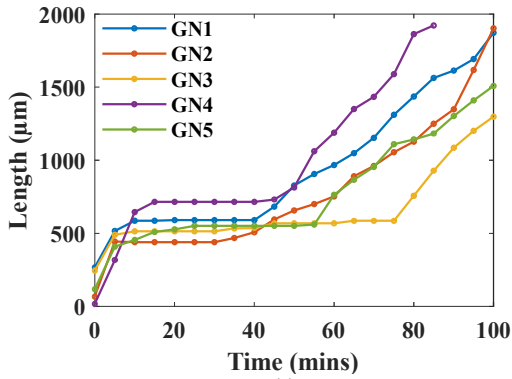


Fig. 3 Growth rate of samples; Length against time are plotted for samples of (a) grounded needle and HV plane and (b) HV needle and grounded plane. Mean (solid lines) and standard deviation (dashed lines) are plotted against time for (c) tree length and (d) tree width.

D. Angle Analysis

The bend and bifurcation angles were measured from the optical images. Bend angles were measured for branches that changed their direction of growth. The outer angle between an initial branch and the successive divided branch was measured as the bifurcation angle.

Angles nearer 180° represent shallow bends or bifurcation deviations. It should be noted that the optical images represent 2D projections of a 3D object, which may lead to an overestimate of smaller angles. However, the measurements were consistent between samples and can thus be used for relative comparison. Normalized (probability) histograms of angle distributions for each sample can be seen in Fig. 4.

The distributions are comparable, suggesting that the electrode which is energized has little influence on the tortuosity of the tree channels.

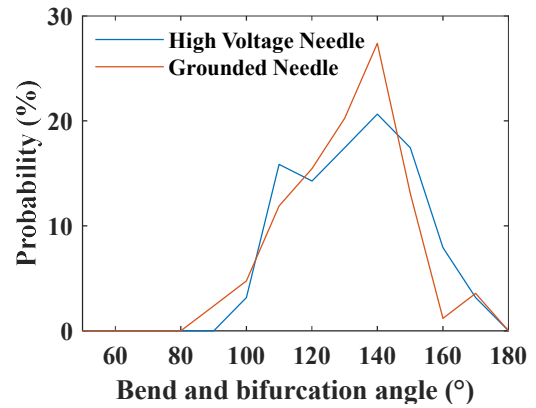


Fig. 4. Histogram of bend and bifurcation angles of all tree samples under HV and grounded needles.

E. Fractal Dimension

Fractal dimension is a measure of the branch density in the 2D image of a tree structure [3]. Table 2 shows a consistent fractal dimension for all samples under HV and grounded needle conditions. The mean fractal dimensions for both configurations are consistent to within one standard deviation, therefore, the relative polarity of the needle-to-plane configuration has a negligible impact on the fractal dimension and branch density of the final tree structure.

TABLE 2: FRACTAL DIMENSION ANALYSIS OF TESTED SAMPLES

Configuration	Sample	Fractal Dimension
HV Needle	1	1.96
	2	1.97
	3	1.97
	4	1.95
	5	1.98
	Mean	1.96
	Standard Deviation	0.01
Grounded Needle	1	1.97
	2	1.97
	3	1.97
	4	1.95
	5	1.96
	Mean	1.97
	Standard Deviation	0.01

F. PD Patterns

The evolution of the PRPD patterns is similar for both datasets. For all samples, in the initial growth period, the PD magnitudes in each phase polarity increase with point-on-phase voltage, sometimes referred to as a “wing-like” pattern as shown in Fig. 5(a). During the stagnant phase, where the tree length does not appear to change through the CCD camera, discharges tend to have smaller magnitudes, which are constant with the phase. Subsequently, when the tree continues to grow, the PRPD pattern shows cyclic magnitude with phase angle, also referred to as a “turtle-like” pattern as shown in

Fig. 5(b). The discharge magnitude is similar for all samples, showing larger magnitudes in the initial growth stages before reducing as tree growth stagnates (Fig. 6). Discharge magnitude then increases as tree growth resumes, but remains at a lower rate than the initial growth stage.

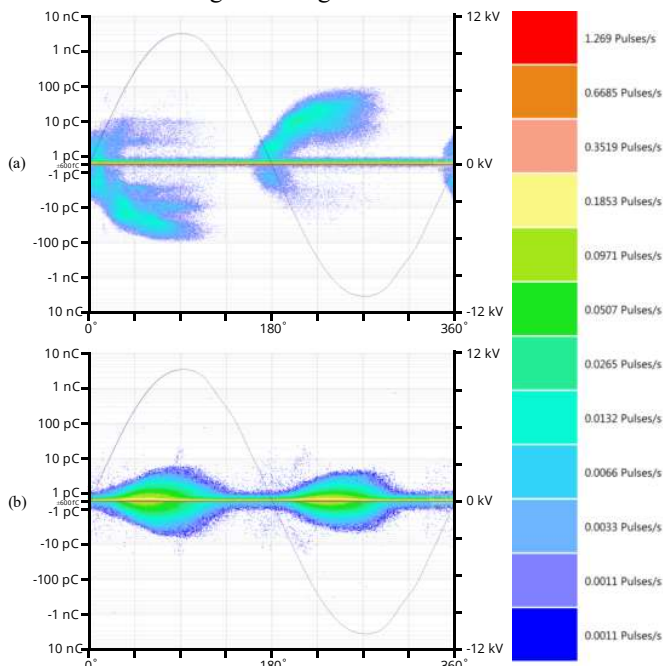


Fig. 5. PRPD patterns tree growth in HV sample 4, representative of PRPD patterns for all samples (a) over a 15-minute interval, starting from initiation in the initial growth stage. (b) Over a 57-minute interval, starting from the secondary growth stage after the stagnant period.

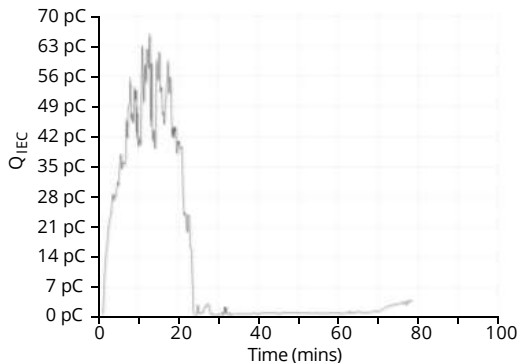


Fig. 6. The trend line of PD magnitude against time for sample no. 4 of the HV needle sample group.

V. CONCLUSIONS

Changing the relative polarity of electrodes had little influence on the electrical treeing properties by the metrics examined in this study, although there is some uncertainty concerning initiation times: Initiation times for grounded needles were observed to be longer than for HV needles. However, a larger statistical dataset is required to draw a more definitive conclusion given its inherent stochastic nature. In needle-to-plane (or similar) electrode configurations, grounded needles can be used to grow electrical trees and these are equivalent to the ones grown with HV needles.

ACKNOWLEDGMENTS

This work was jointly funded by the EPSRC Supergen Offshore Renewable Energy Hub [grant number: EP/S000747/1] and Offshore Renewable Energy Catapult Ltd. The authors would like to thank Dr. Fang Liu for valuable discussion and Mr. Morris Patterson for experimental support.

For the purpose of open access, the author has applied a CC BY public copyright license to any Author Accepted Manuscript version arising from this submission.

REFERENCES

- [1] N. Shimizu and C. Laurent, “Electrical tree initiation,” *IEEE Trans. Dielectr. Electr. Insul.*, vol. 5, no. 5, pp. 651–659, 1998.
- [2] Z. Lv, S. M. Rowland, S. Chen, H. Zheng, and I. Idrissu, “Evolution of partial discharges during early tree propagation in epoxy resin,” *IEEE Trans. Dielectr. Electr. Insul.*, vol. 24, no. 5, pp. 2995–3003, 2017.
- [3] K. Kudo, “Fractal analysis of electrical trees,” *IEEE Trans. Dielectr. Electr. Insul.*, vol. 5, no. 5, pp. 713–727, 1998.
- [4] H. Zheng, G. Chen, and S. M. Rowland, “The influence of AC and DC voltages on electrical treeing in low density polyethylene,” *Int. J. Electr. Power Energy Syst.*, vol. 114, pp. 1–13, Jan. 2020.
- [5] G. Chen and C. H. Tham, “Electrical treeing characteristics in XLPE power cable insulation in frequency range between 20 and 500 Hz,” *IEEE Trans. Dielectr. Electr. Insul.*, vol. 16, no. 1, pp. 179–188, 2009.
- [6] D. W. Kitchin and O. S. Pratt, “Treeing Effects in Polyethylene,” *Electrical Engineering*, IEEE, pp. 218–223, Mar. 1958.
- [7] J. H. Mason, “Assessing the resistance of polymers to electrical treeing,” in *IEE Proceedings A (Physical Science, Measurement and Instrumentation, Management and Education, Reviews)*, 1981, pp. 193–201.
- [8] A. B. Johansson, A. B. Sandberg, B. Sonerud, J. H. M. Blennow, and S. M. Gubanski, “Wire-Plane Electrode System for Electrical Tree,” 2011.
- [9] Y. Liu, X. Cao, and G. Chen, “Electrical tree initiation in XLPE cable insulation under constant DC, grounded DC, and at elevated temperature,” *IEEE Trans. Dielectr. Electr. Insul.*, vol. 25, no. 6, pp. 2287–2295, 2018.
- [10] BSI Standards Publication, “High-voltage test techniques. Partial discharge measurements, BS EN 60270:2001+A1:2016, IEC 60270:2000,” 2001.
- [11] J. H. Mason, “Breakdown of solid dielectrics in divergent fields,” *Proc. IEE Part C Monogr.*, vol. 102, no. 2, p. 254, 1955.
- [12] H. Zheng, S. M. Rowland, and N. Jiang, “Influence of electrode separation on electrical treeing in a glassy epoxy resin,” *Annu. Rep. - Conf. Electr. Insul. Dielectr. Phenomena, CEIDP*, vol. 2017–Octob, pp. 769–772, 2018.
- [13] L. A. Dissado and J. C. Fothergill, *Electrical Degradation and Breakdown in Polymers*. 1992.